

Ultrasound in Medical Imaging: Wave shaping

BY M. K. COWAN

From detecting deadly submarines in the First World War, to giving parents the first images of their new child, ultrasonic imaging has been one of the most elegant technologies to emerge from the twentieth century. While sonic imaging finds uses across all fields, from precise picosecond pulse-probe imaging of semiconductor quantum structures (with nanometre resolution) to somewhat crude proximity detectors (a cheap and common project for the electronics hobbyist), its most widely known application is undoubtedly in medical imaging.

While many technologies exist with advantages over ultrasound, such as the ability of MRI (magnetic resonance imaging) to non-invasively image deep into bone structures (virtually unreachable with ultrasound), or that of nuclear medicine to image the transport and accumulation of select substances within the body, none of them can match the simplicity, safety and convenience of ultrasonography. Ultrasound requires no ionising radiation, no dedicated room and minimal preparation. While there are known risks to ultrasonic imaging, they are considerably less common and less dangerous than the risks associated with many other imaging technologies and techniques; the lack of ionising radiation also allows ultrasound examinations to be repeated frequently, with no known cumulative risk to the patient.

In this document, I will present an overview of medical ultrasound technology with a brief history and a comparison to other medical imaging technologies and certain non-medical imaging technologies from which ultrasound imaging borrows many concepts.

Contents

| | |
|--|-----------|
| 1. Introduction..... | 2 |
| Out of the bat-cave | 3 |
| An invention of Titanic proportions | 3 |
| Medical Ultrasound | 4 |
| Pulse-echo principle | 4 |
| Time selection | 4 |
| Depth-selection | 4 |
| Thought experiment: Shutter & flash..... | 5 |
| 2. Display modes | 6 |
| Amplitude (A-mode) | 6 |
| Brightness (B-mode) | 6 |
| Motion (M-mode) | 7 |
| 2D real-time (RT) | 7 |
| Doppler modes..... | 7 |
| Continuous wave Doppler | 7 |
| Pulsed Doppler..... | 9 |
| Colour Doppler..... | 9 |
| 3. Arrays and scanning | 10 |
| Linear and curvilinear arrays | 10 |
| Side-lobes | 12 |
| Phased arrays..... | 12 |
| Depth-selection by focusing: A practical demonstration | 14 |
| Multiple-zone focusing..... | 15 |
| Parallel beam forming | 15 |
| Dynamic depth focusing | 15 |
| 4. 3D/4D Ultrasound | 15 |
| 5. Conclusion | 16 |
| 6. Table of figures..... | 17 |
| 7. References | 18 |

1. Introduction

From the echolocation techniques employed by James Holman (the “Blind Traveller”) on his voyages in the early 19th century, to the submarine-detecting sonar (sound navigation and ranging) used during the world wars, sound has been used extensively to image in situations where imaging with light would be impracticable or impossible. In the late 19th century, Lord Rayleigh published “the Theory of Sound”, describing the wave-nature of sound

and thus allowing optical imaging techniques to be applied to acoustic imaging*. Imaging methods for both the near and far fields can utilise sound instead of light, and some more exotic techniques such as pump-probe and nonlinear propagation may use acoustic waves instead of electromagnetic waves.

* Also explaining how humans naturally localise sound sources, in his *Duplex Theory*.

Out of the bat-cave

At the end of the 18th century, Lazzaro Spallanzani investigated the peculiar ability of bats to navigate in dark caves without crashing into one another (or indeed the cave itself). From this, came the discovery of ultrasound – sound with frequencies above the range of human hearing (commonly defined as 20 kHz). In addition to seeing their surroundings by detecting light that enters their eyes, bats* also emit pulses of ultrasound, and listen for the reflected sound (echoes). As sound in air travels at around 300 metres per second, every millisecond between the pulse and an echo represents an extra fifteen centimetres between the bat and the reflecting object (approximately). The wavelength of ultrasound is generally below fifty microns, as any greater would place the sound in the human hearing range (thus “ultrasound” would cease to be an accurate description of it), so even low-frequency ultrasound (several tens of kilohertz) can provide sub-millimetre depth resolution.¹

An invention of Titanic proportions

After the sinking of the Titanic in the early twentieth century, an interest suddenly emerged amongst inventors for a device that could detect icebergs when visibility was poor. Sound was particularly well suited for this task, as sound travels approximately five times faster in water than in air (near sea level), allowing echoes to be received quicker. Within weeks of the sinking, a patent had been filed for an underwater echolocation device, with the first such device being built by Reginald Fessenden. Early sonar had poor resolution and was more of a proximity sensor than an imaging technology, due to the relatively low sound

frequencies available (with electromagnetic transducers) and the lack of signal-processing technology at the time. The First World War however resulted in a lot of money being invested in sonar, and with the advancement of electronic amplifiers[†] and the integration of piezoelectric transducers[‡], it was only four years after the sinking of the Titanic when a the first German U-boat was sunk due to detection by sonar.¹

In addition to developing an early sonar-driven iceberg-detection device, Fessenden also advanced the wireless communication technology pioneered by Marconi, explaining the wave-nature of the signals used in long-range two-way radio communication[§]. With the increased use of aircraft during the Second World War, and sound-based aircraft detectors being very prone to interference from ground sources², a similar technology (also based on the pulse-echo principle) that utilised radio waves was developed. Radio detection and ranging technology^{**} (RADAR, first demonstrated in 1935) received considerable military attention. In addition to detecting aircraft and estimating their distance (ranging), the Doppler shift was utilised to estimate the speed of the aircraft (resolved along the radar station’s line-of-sight). Various techniques were employed to allow the radars to “scan” different angles, providing 2D images. While ultrasound did not receive as much attention during the Second World War, the similarities between acoustic and radio imaging allowed advances in radio (and

[†] Due to the invention of the vacuum tube, the predecessor to the modern field-effect transistor (although the semiconductor FET was not the first solid-state transistor to be created).

[‡] Discovered over thirty years before the war.

[§] Contrary to the “whiplash” theory accepted by most scientists of the time, including Marconi.

^{**} Although the original idea had been to use radio waves to melt aircraft or to incapacitate the pilot – the “death ray” previously proposed by Nicola Tesla.

* Over half the known species of bat:

<http://www.scientificamerican.com/article.cfm?id=how-do-bats-echolocate-an>

microwave) imaging to find their way into ultrasonic imaging over time. After the war, many countries released details of, or began to develop technologies for non-destructive testing* that employed ultrasound.¹

Medical Ultrasound

George Ludwig experimented with using industrial ultrasound on various animal tissues and organs. In addition to realising that different organs and structures had varying acoustic impedances (allowing them to be detected by reflected sound), he also determined the average speed of ultrasound in soft tissues, to be (on average) 1540 ms^{-1} , a value which is still used as standard today.¹ He also experimented with different ultrasound frequencies. Lower frequencies cannot image small details, due to the Rayleigh criterion, whereas higher frequencies are absorbed more strongly by soft tissue (greater attenuation coefficient), resulting in a loss in imaging depth.³

Pulse-echo principle

Time selection

In the late 19th century, Eadweard Muybridge was hired to answer a much-debated question:

“When a horse gallops, are all four hooves off the ground at the same time at any point during a gallop?”

Muybridge placed a series of cameras along a track (at 21-inch intervals), and triggered them with a pulled string, such that they would be triggered with a short time delay ($\sim 1 \text{ ms}$) between each successive shoot.⁴ This resulted in a series of photos, representing different stages of the horse's gallop:

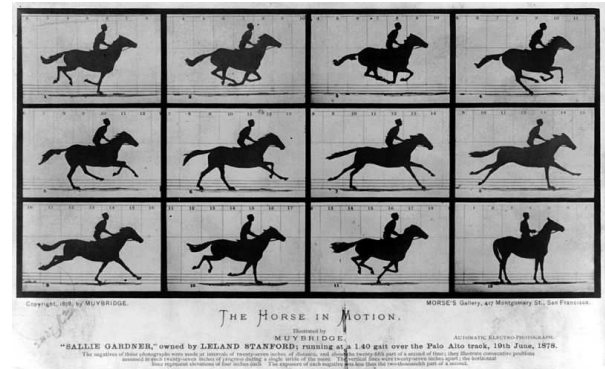


Figure 1: "The Horse in Motion", Eadweard Muybridge, possibly the first example of a video recording.⁵

Depth-selection

The subject of Muybridge's photographs was illuminated by the ambient light (presumably daylight) at the track. If the camera was also to provide the illumination, it would record the reflected and back-scattered light from the subject. In this configuration, the camera is essentially recording optical echoes (reflections).

If the illumination source could be pulsed (a fast flash), echoes from surfaces further from the camera would take longer to reach the camera, as they would have a longer distance to travel. If we could set the shutter to open for a controllable (and short) amount of time, at a precise time after the firing of the flash, we could record reflections that originated from a certain distance from the camera.

If we were to set up many cameras with a short delay between the shutters on each one, similar to Muybridge, but have a single flash as the only source of illumination, we could record a series of depth cross-sections – with cameras that were fired earlier recording details of the scene that were closer to the illumination and cameras. Time-selection in combination with a pulsed light source, allows selection of an imaging depths.

* For example, scanning for defects in sheets of metal intended to be used in the hulls of ships.

Thought experiment: Shutter & flash

Consider the following (Figure 2):

- Bounce a wave off a surface 50cm away
 - » 50 cm out + 50 cm back \rightarrow 100 cm path length
- Detect the back-reflected wavefront. The shape of the reflected wavefront gives information about the surface relief of the object.
 - » 5 mm bump \rightarrow 1% change in path length.
- What time-resolution (shutter rate) is needed to detect a 5mm bump?
 - » 5 mm bump \rightarrow 1% change in path length.
- Assuming a perfect sensor and emitter, what bandwidth is required to transmit information to a computer, from a single sensing element?
 - » Perfect: zero rise and fall time
 - » Assume poorest dynamic range (1-bit: high/low only)
- Light travels one metre in 3ns
 - » 5 mm detail \rightarrow 30 ps time-shift
 - » Very fast transducer required
 - » 30 ps \rightarrow 30 GHz
 - » Very fast electronics required
 - » 30 Gbit/s bandwidth: the maximum bandwidth of a high-end PC graphics card link (32 Gbit/s for 16-lane PCI Express) - per sensing element
- Sound (in air) travels one metre in 3ms (~ 0.2 ms in soft tissue)
 - » 5 mm detail \rightarrow 30 μ s time-shift
 - » 30 μ s \rightarrow 30 kHz
 - » High-speed electronics not necessary: the oscillator in a quartz wristwatch has a frequency of around 32 kHz; the average PC sound card can sample at over 40 kHz. For a 0.5 mm detail (3 μ s time-shift), a 555 timer (very cheap, popular with hobbyists) is capable of timing down to microseconds⁶.
 - » 30 kbit/s: a hundred such elements could share a single Bluetooth link
 - 450 kbit/s for imaging in soft tissue – less bandwidth than a digital radio station.

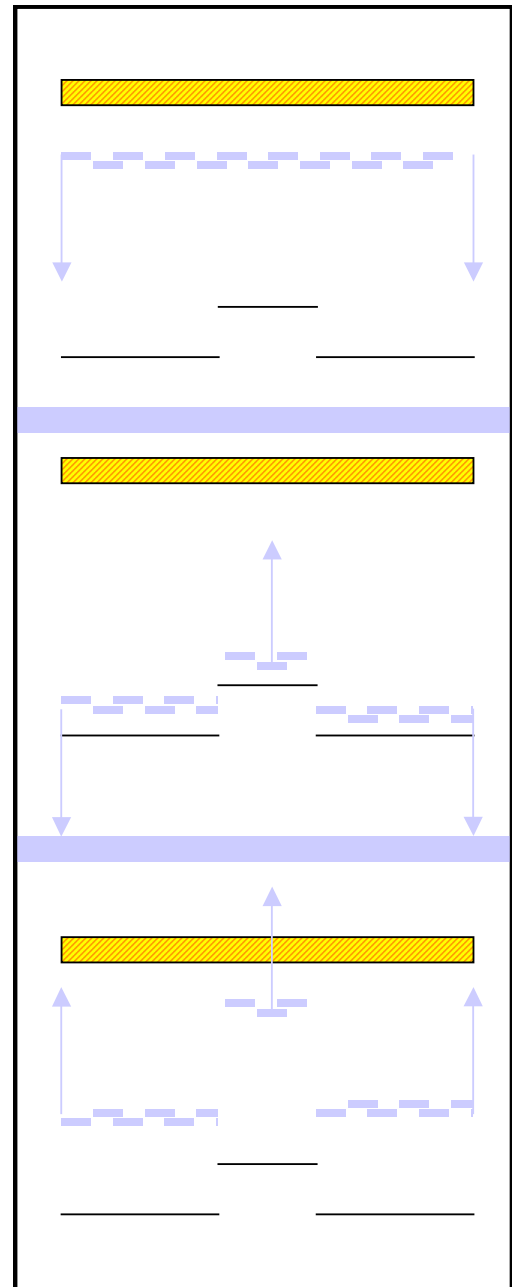


Figure 2: Pulse-echo - reflecting a wavefront off a surface, then detecting the deformed wavefront in order to calculate the relief of the reflecting surface.

This demonstrates the practicality of using sound to image features within the human body – organs and blood vessels will typically be millimetres to centimetres in size and in thickness.

2. Display modes

Various different visualisation methods are employed in ultrasound imaging. Some existed only due to the technological limitations of their time (ultrasound imaging pre-dates the solid-state digital computer), while others emerged as necessities in order to present new kinds of data such as motion.

Amplitude (A-mode)

Initially, a single transducer was used, to create a 1D image of reflections originating from different depths (distances from the transducer). Acoustic lenses could be used to taper the pulses, widening or narrowing the imaging field. High intensity ultrasound, particularly with frequencies on the order of 100 kHz, was also used to destroy tumours.

Pulses of ultrasound would be emitted at regular intervals, and the echoes would be plotted on a waveform-style display⁷, similar to a CRT oscilloscope:

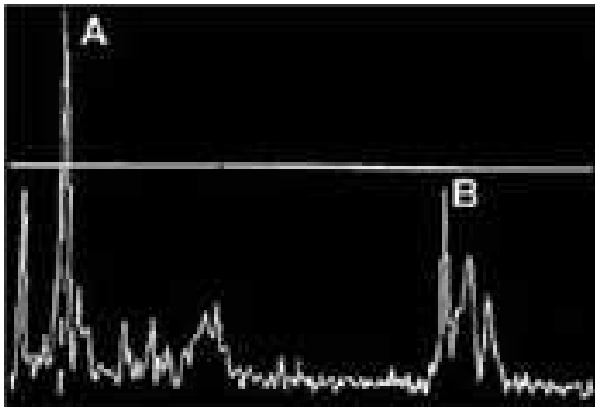


Figure 3: A-mode ultrasound output⁸.

The CRT scan is synchronised to start every time an ultrasound pulse is emitted. Distances along the x-axis represent time (in the recorded signal), which corresponds to distance along the imaging line (depth). The y-axis corresponds to the amplitude of the signal measured at the detector at that time. While this method provides a simple image, it is not particularly easy to interpret. As the energy of an

ultrasound pulse will be absorbed as it passes through tissue (and converted to heat), some form of amplification is often applied to the received signal, with increasing gain as time progresses (until the next pulse, where the gain is reset back to minimum). This is known as time-gain compensation, commonly abbreviated to TGC.

Brightness (B-mode)

Brightness mode improves on the readability of the output, by displaying the received signal as a 1D line of points (the x-axis), with the brightness of each point corresponding to the intensity reported by the detector/transducer. By scanning the beam at different angles, or by use of an array of transducers, a 2D image may be produced:

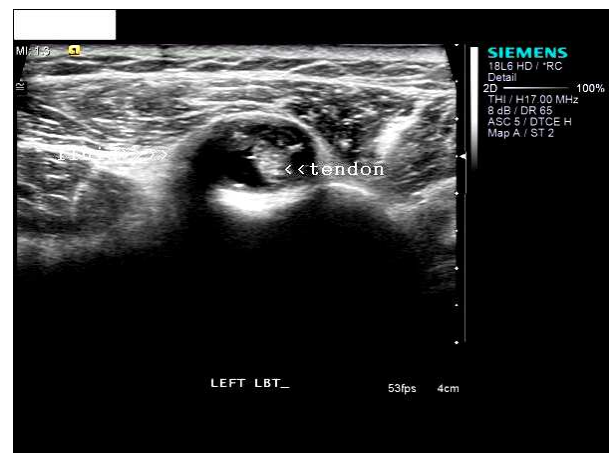


Figure 4: B-scan of an inflamed bicep tendon⁹.

“Compound” B-mode utilises several B-mode scans from different directions, and computes the object from a series of images. This avoids the “shadows” that bones and air-gaps* and other strong reflectors and scatterers may create, in addition to various other artefacts.

Various methods of scanning beams and various array geometries exist, each with their own strengths and weaknesses. These will be discussed in the next chapter.

* For example, the airways and lungs

Motion (M-mode)

Motion-mode imaging is useful for imaging movement, particularly of heart structures. This operates similarly to single-element B-mode, however successive scans are stacked next to each other. Hundreds of scans per second are possible, allowing temporal resolutions on the order of milliseconds to be realised. In addition to displaying the motion of various structures, it also allows the size of moving structures (e.g. heart valves, heart wall) to be measured:

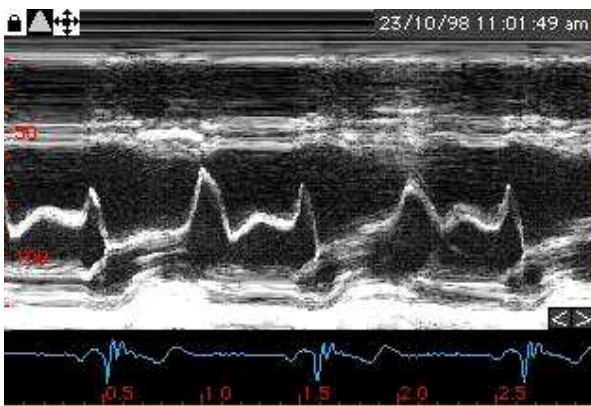


Figure 5: M-mode mitral valve¹⁰

2D real-time (RT)

In a similar way as to how the progressive capture of still images enables the realisation of motion-capture, successive B-mode scanning can produce “ultrasound video”. As the recording of a single frame requires transducers and processing equipment capable of sub-millisecond temporal resolution, high frame rates (on the order of hundreds of frames per second) are possible. The main upper limit on the frame rate is the loss of depth associated with the shorter available time to listen for echoes during the recording of each frame, before the pulse for the next frame must be sent.*

* Motion ultrasound cannot be demonstrated particularly well on paper, a good example of real-time ultrasound imaging is available at:

<http://www.frca.co.uk/images/EnVisorMe600010032.gif>

Doppler modes

The similarities between acoustic and radio imaging extend beyond basic photographic concepts. The Doppler shift (Figure 6) of pulses reflected from moving objects may be measured, and displayed on a B-scanned image (commonly as colour), displayed by itself as a graph of Doppler shift over depth, or presented acoustically.¹²

$$\delta f = f_d - f_0 = \left[\frac{c \pm v}{c \mp v} - 1 \right] f_0 \cos \theta \approx 2vf_0 \cos \theta / c$$

Figure 6: Doppler shift for frequency f_0 , when reflected from an object moving at angle θ with respect to the pulse direction, and at velocity v through a medium where the pulse propagates at speed c . The pulse is shifted from frequency f_0 to f_d . This equation assumes that the transmitter and the receiver are stationary with respect to the medium.

Continuous wave Doppler

Separate transmitter and receiver elements are used, in order to provide continuous wave ultrasound “illumination” of area of interest. Ultrasound reflected back from stationary surfaces and scatterers will not be Doppler shifted and may be filtered out, however reflections from moving interfaces (e.g. some blood moving along an artery) will return a Doppler shifted signal. The returned signal is commonly combined with part of the original in a non-linear mixer (such as a ring modulator), which produces additional frequencies, equal to the sum and the difference between the originals†. This mix is then passed through a low-pass filter, which removes the original wave, the Doppler shifted wave and the sum, leaving a frequency equal to the Doppler shift. While a spectrum analyser can give a precise indication of the various velocities of bodies in the acoustic field, for simple analysis of blood flow the low-pass filtered output may be played

† Commonly known as self-heterodyne mixing

back through loudspeakers.¹² For example, to monitor blood flow in the carotid artery:

- Assume ultrasound frequency $f_0 = 3 \text{ MHz}$
- Blood maximum velocity¹¹ $v_0 \approx 0.5 \text{ ms}^{-1}$
- Speed of sound in tissue $c \approx 1540 \text{ ms}^{-1}$
- Measured at an angle $\theta = 20^\circ$ to the flow

The output from the low-pass filter, equal to the Doppler shift, is given by:

$$\begin{aligned}\delta f_0 &\approx 2vf_0 \cos \theta / c \\ &= 2 \times 0.5 \times 3 \times 10^6 \times \cos 20^\circ / 1500 \\ &= 820 \text{ Hz}\end{aligned}$$

This is within the range of human hearing* (20–20,000 Hz), allowing primitive blood flow measurements to be made without the need for a graphical display (thus allowing the equipment to become extremely compact and portable). A major disadvantage of this method however is that no image is obtained.

As objects moving with different velocities will produce different frequency “notes” in the filtered output, a spectrogram may be produced, displaying the relative intensities of different frequencies at different moments in time.¹² An envelope may be overlaid on the spectrograph, showing the maximum frequency with intensity above some threshold at each moment in time, allowing the signals from the fastest objects to be identified quickly.

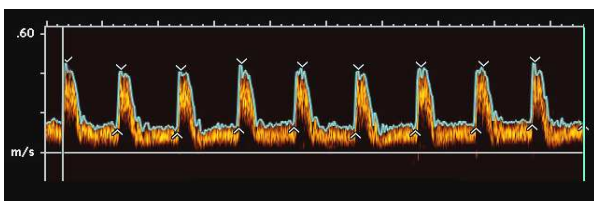


Figure 7: Doppler spectrum¹² with envelope

Slower-moving objects that may contribute to the spectrogram include the walls of blood vessels, expanding and contracting with the pressure of the passing blood; arteries also have a muscular layer around them to pressurise the

blood as it passes through. We can take a single time-slice through the spectrum and display it as amplitude vs. frequency, in order to separate the different moving objects (by velocity) at that time:

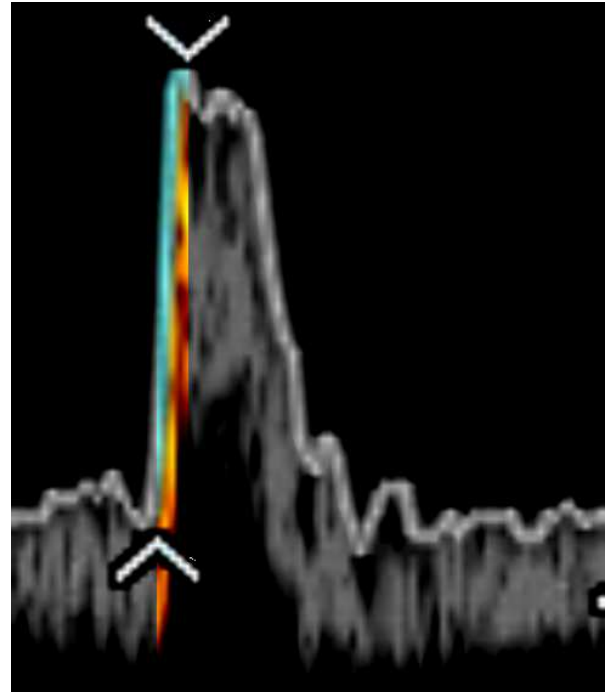


Figure 8: Taking a time-slice through a Doppler spectrum

This slice may then be transformed to a graph of intensity vs. frequency, which corresponds to the amount of energy reflected from objects moving with various velocities:



Figure 9: An intensity plot of a time-slice through the Doppler spectrum in Figure 7/Figure 8 is shown. The y-axis represents the Doppler shift and the X-axis is the intensity of reflected sound at that frequency. Notice that there are a variety of different velocities being reported, the values of which may be estimated from the y-axis labels in Figure 7

* Slightly more than one and a half octaves above the middle-C on a piano

Continuous-wave Doppler does not provide an image (a continuous wave contains no timing information), and requires the angle between moving bodies and the transducers to be known already. It is however a simple and compact way to monitor the flow through larger blood vessels (e.g. the jugular vein), where the angle can be estimated.

Pulsed Doppler

By pulsing the transmitter, we may produce an image. We may also use a single transducer to transmit and to receive, as simultaneous reception and transmission aren't necessary. This ability to obtain an image in addition to velocity information is very useful: estimation of the flow angle is no longer required, as the blood vessel of interest will be shown in the image, allowing its angle relative to the pulses to be deduced. The image also allows the operator to see if any other blood vessels are near the one of interest – other flows in the imaging field will add to (and smear) the velocity profile. The velocity profile and image are typically both displayed alongside each other, and the operator can “draw” a line along the blood vessel of interest on the image, to allow the computer to adjust the velocity profile to account for the imaging angle:



Figure 10: Pulsed Doppler: Image and velocity information. The operator can use the image to indicate the flow angle to the computer.¹²

Colour Doppler

If the receiver can determine the lateral location (in addition to the depth) of a reflecting source, why not apply the same processing to determine the location of a moving source? In colour Doppler, a spatially resolved velocity profile is overlaid as colour onto the intensity profile obtained from B-mode scans. This allows the velocity field to be displayed:

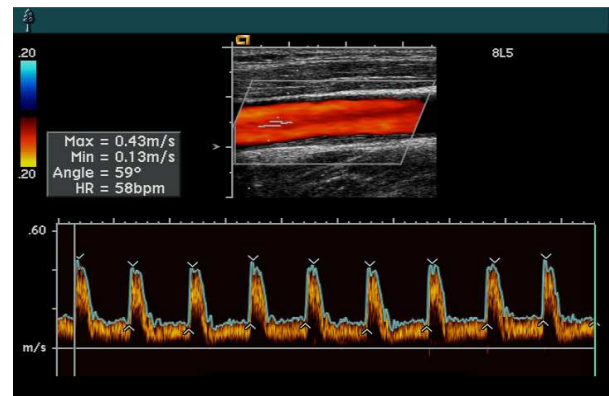


Figure 11: Colour Doppler. A B-mode image is displayed above, with the velocity field superimposed as artificial colour. The scale on the left indicates the colour used for various velocities. The velocity spectrum is displayed below the image.

Colour Doppler can only show one velocity for each location, so typically the maximum, minimum or mean velocity within each unit area is displayed. Extra velocity information may be displayed separate to the image, as is shown in Figure 11.

3. Arrays and scanning

A single transducer can obtain a 1D image, and optionally, velocity information (via pulsed Doppler). In order to produce a 2D (or 3D) image, we need some way to “scan” the ultrasound pulses laterally. This could be done by mechanically moving the transducer after each individual scan, to produce several “columns” of image data (with each column representing depth information obtained at a particular transducer location). This is slow, as mechanical movement is required, so any movement of the patient will reduce the image quality, and Doppler techniques will not translate easily into this scanning method, due to the large delays between successive scans, as the transducer is moved.

Linear and curvilinear arrays

Instead, we create an array of transducer elements, side-by-side. As soon as one has finished imaging the column of tissue below it, the next element can be fired without the delay that would be incurred by mechanical scanning. This simple row of transducer elements is commonly referred to as a *linear array* (pictured below):



Figure 12: A linear array¹³

The imaging field of a linear array is somewhat limited, as it can only image in lines perpendicular to the array surface, so the lateral extent of the imaging field is similar to the dimensions of the array.

In order to widen the imaging field (at the expense of lateral resolution), an acoustic lens may be employed or (more commonly) the elements may be angled in such a way as to create a curved surface at the front of the array:



Figure 13: A curvilinear array

To increase the imaging depth, we increase the time between pulses, at the expense of image acquisition speed. To increase the depth resolution, we use faster transducers and electronics.

Note that some strongly reflecting or strongly absorbing materials (e.g. bone, gas bubbles) will not allow a sufficient amount of ultrasound to pass through for imaging beyond them. This results in shadows being cast by such objects, with no information available about the structures within or beyond them.

To increase the lateral resolution, can we simply increase the density of transducer elements? What limits the achievable lateral resolution? As the element density increases, the element size decreases – how does this affect the beam shape, with regards to the Fresnel and Fraunhofer regimes (Figure 14)?

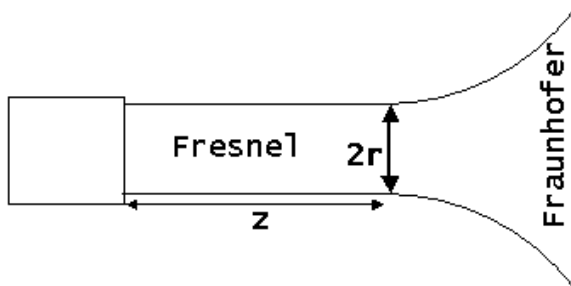


Figure 14: Near field (Fresnel) regime of length z , from transducer element with radius r , and far field (Fraunhofer) regime.

- Assume 50 elements on 5 cm array – so element radius $r = 0.5$ mm
- Speed of sound in:
 - » Air: $v \approx 300$ m/s
 - » Tissue: $v \approx 1500$ m/s
- Ultrasound at 3 MHz:
 - » $\lambda \approx 0.1$ mm (air)
 - » $\lambda \approx 0.5$ mm (tissue)
- What limits our imaging in the near field?
 - » Near-field (Fresnel) length ($z = r^2 / \lambda$)
 - $z \approx 2.5$ mm (air)
 - $z < 1$ mm (tissue)
 - » Depth of near field reduces as the element density increases.
- Near field does not penetrate very deeply. Can we image with far-field reflections?
 - » Far-field (Fraunhofer) divergence in tissue:
 - $\theta = \sin^{-1}(1.22\lambda / 2r) \approx 35^\circ$
 - » Cannot image in far-field with this array as the pulse diverges rapidly ($\sim 70^\circ$ cone angle)

As the element density increases, the near field length decreases and the far field divergence increases. Therefore, increased lateral resolution (by using smaller elements) is achieved with a decrease in imaging depth.

A simple, but effective solution to this compromise is to fire several adjacent elements simultaneously, emulating a single larger element. This allows the position of the pulse-centre to be precisely controlled, as a multiple of the element width, while still maintaining a large aperture size (the width of the emitted pulse). A single array may therefore be electronically reconfigured to provide wider pulses for imaging deeper, or narrower ones for increased lateral resolution, as illustrated by Figure 15 and Figure 16:

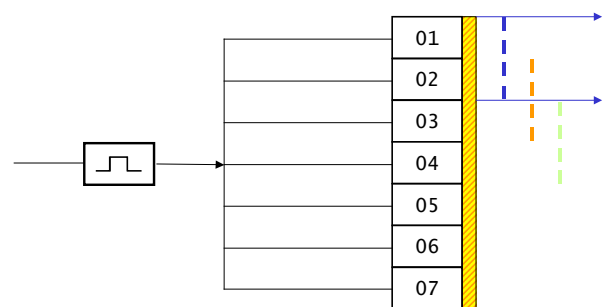


Figure 15: A linear array where adjacent elements are fired in groups of two. Six groups are possible on the illustrated array, allowing the near-field depth to be quadruple that of a single-element array, while only reducing the lateral resolution by $1/7$ (14%)

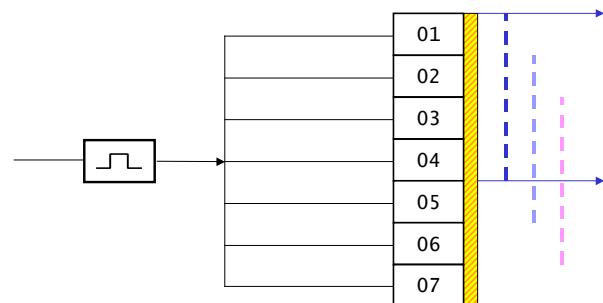
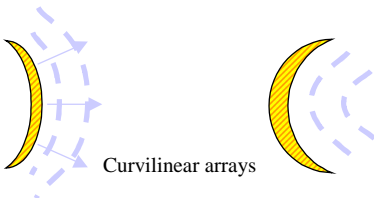
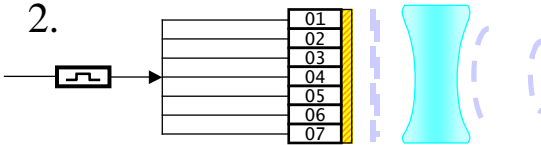


Figure 16: A linear array where adjacent elements are fired in groups of four. Four groups are possible on the illustrated array, allowing the near-field depth to be sixteen times that of a single-element array! The lateral resolution however has been reduced by $3/7$ (42%), although a typical array would have considerably more than seven elements!

Phased arrays

With linear and curvilinear arrays, we have produced flat wavefronts from transducers, and then tried to reduce diffraction effects[†] (e.g. Fraunhofer diffraction) by firing multiple elements at once, or using acoustic lenses (Figure 18). If we could shape the wavefronts instead, this would allow lenses to be simulated, by producing wavefronts that were shaped as if they had already passed through lenses.

1.  Curvilinear arrays

2. 

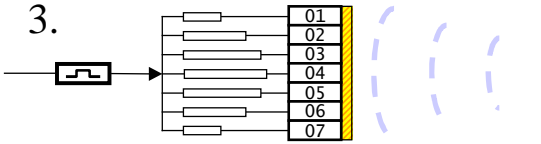
3. 



Figure 17: Side-lobes – notice the dark “bowel-like” structures [follow green arrows], produced by the side-lobes reflecting off the actual bowel [imaged at the purple arrows].¹⁶

Figure 18: Wavefront shaping by (a) shaped arrays, (b) acoustic lens and (c) phased array (boxes represent delay)

* Which has received a considerable amount of military attention and thus, funding!

† Side-lobes will not be discussed in this document, however they are essentially higher order diffraction maxima of the transmitted beam, due to each source (transducer) also behaving as an aperture.

Phased arrays electronically delay the signals to and from the transducers, to account for the different path lengths between each transducer and the area of interest:

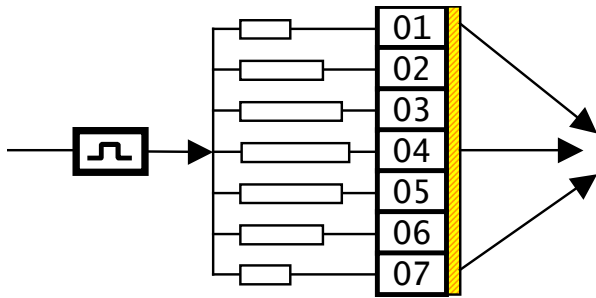


Figure 19: Phased array focusing the pulse.

A delay is applied to all the elements. As all the elements may be fired simultaneously, this configuration has a greater signal to noise ratio and can image structures at considerable depth, compared to linear arrays that fire subsets of the array. In Figure 19 the central elements have a larger delay, to account for the shorter path length between them and the region of interest. As the outer regions of the produced wavefront will be spatially ahead of the more central regions, this results in a curved wavefront, as if a plane wave had been focused by a lens. The same delay is applied to the received signals, and spatial coherence between the signals received by different elements indicates the presence of some reflecting or scattering structure in the focal plane. The focal distance can be increased by increasing the curvature of the wavefront, and may be decreased by decreasing the curvature.

In addition to allowing the array to focus to a particular depth, an asymmetric delay profile may be used to sweep the focal point laterally. This allows the entire array to be used to image points off the central axis of the array (Figure 20) and even completely out of the volume that would be accessible with a linear array (Figure 21).

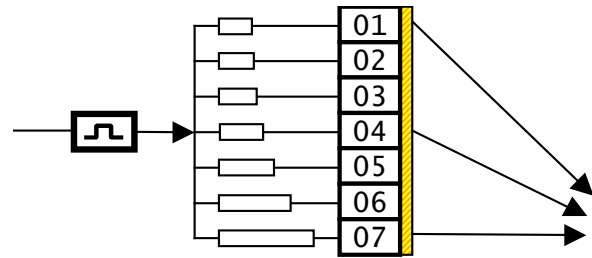


Figure 20: Sweeping the beam with a phased array, by introducing an asymmetric delay to the transducers in order to shape the wavefront.

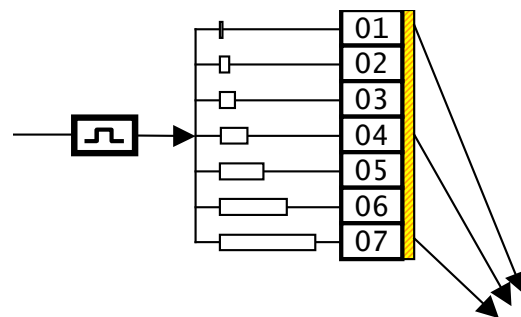


Figure 21: Off-axis imaging with a phased array.

Phased arrays can look “around” obstructions such as bone and gas gaps as the same spot can be imaged from various directions by beams originating from different regions of the array. By averaging scans taken from different directions, noise due to physical and electrical limits may be cancelled out in addition to removal of “speckle” noise^{*,14,17}. Additionally, a 2D arrangement of transducers (Figure 22) may be used to obtain a full 3D image.



Figure 22: A 2400-element 2D phased array.¹⁸

* Speckle is due to scatterers smaller than the sound wavelength. It is deterministic so a simple repeat-and-average approach will not remove it.

Depth-selection by focusing: A practical demonstration

Depth selection by focusing may be demonstrated with an average compact digital camera and objects placed at different distances from it. In the first image (Figure 23), the digital camera is focused on the box camera (accounting for the focusing effect of the magnifier); the magnifier is almost unnoticeable (if not for its frame, then a few specular reflections off the lens). In the second image (Figure 24), the camera is focused on the lens surface, showing clearly the scratches and dust on the lens but with the box camera rendered almost unidentifiable.



Figure 23: Depth selection by focusing. The box camera is in focus; the lens surface is not. The rough surface of the box camera is clearly visible.



Figure 24: Depth selection by focusing. The lens surface is in focus; the box camera is not. The dirt on the lens is now clearly visible, while the camera is reduced to a dark blur.

The lens-aperture system simulates an aperture the size of which varies with the distance that it is viewed from. The effective aperture “shrinks” as the viewer moves further from the focal plane. This results in the system behaving as an optical low-pass filter, where the cutoff frequency decreases for objects further from the focal plane. The point-spread function of the system grows wider when the object is “out of focus”. A high-pass filter is applied to both the images, and the result is shown below, showing the “variable lowpass filter” analogy of the lens-aperture system:

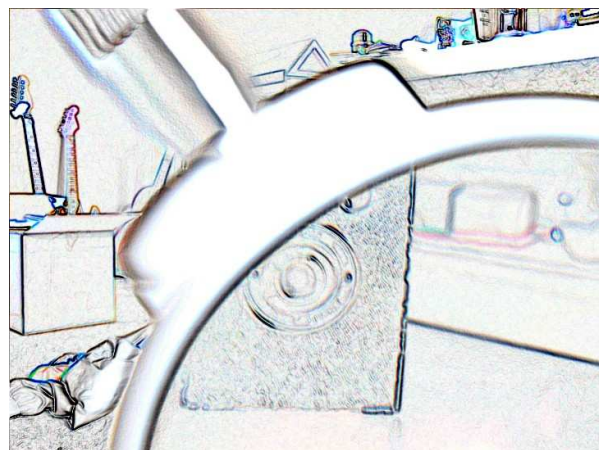


Figure 25: High spatial frequencies were only recorded when they originated from near the focal plane. Hence the most detail in this filtered image is on the camera and guitars.



Figure 26: The details of the box were filtered by the focusing of the camera, now the only visible details are in the new focal plane - the lens surface.

Multiple-zone focusing

The focal point may be moved closer to and further from the scanner, in order to build an image of the structures directly below the transducer. The beam may then be swept to a different angle, and another depth column can be recorded. By using sections of the array instead of the whole array, intersecting columns at a variety of angles may be recorded, and combined to produce a 3D image, with extra clarity around the point of interest due to the columns overlapping at and near it. This process results in a lower frame rate than 2D real time imaging, as different depths must be probed separately, however the spatial resolution at more distant depths is improved by the focusing of the array, partially overcoming beam-widening diffraction effects.

Parallel beam forming

Just as a camera may be focused onto a certain depth, despite the light source (ambient or flash) not being focused, a phased array may be focused to receive, while unfocused to transmit. This allows several sections of the array to focus on different locations simultaneously, increasing the speed at which a full frame can be obtained, by receiving several columns concurrently:

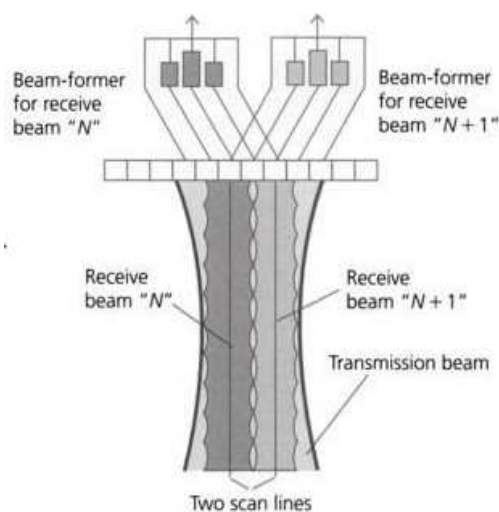


Figure 27: Dynamic Depth Focusing¹⁹

Dynamic depth focusing

Echoes from a certain depth will take the same amount of time to return to the array regardless of the array focusing*. Therefore, we can image an entire column in one pulse with a phased array, by varying the focal length of the array with time, after the pulse has been emitted. As time progresses, the focal length increases, as the depth of detectable reflecting structures will increase with time – due to the increase in path length corresponding to the longer echo delay.²⁰

4. 3D/4D Ultrasound

The arrays that have been described so far produce 1D and 2D images. By combining several such arrays to form an “array of arrays”, i.e. a grid of transducer elements, several 2D slices may be obtained, and layered to form a 3D image. Phased-array techniques may be applied to this array of arrays (synthesising a 3D wave instead of the previously described 2D wavefronts), allowing 3D focusing of the array. Advances such as parallel beam forming and dynamic depth focusing allow full 3D images to be obtained several times per second, allowing a 3D video to be recorded, commonly termed 4D ultrasound. 3D ultrasound may be displayed as a series of “slices”, of increasing distance along one lateral axis.

* Focusing does not affect the speed of sound in the medium!

5. Conclusion

Ultrasound imaging is an incredibly versatile technique allowing non-invasive imaging of soft tissue structures and capable of millimetre resolution at depths of a couple of centimetres. The simplicity of the electronic and computer technologies involved, and in the underlying theory (in contrast to MRI and OCT) allows ultrasound-imaging devices to be portable, compact*, durable and simple to operate (compared to other 3D imaging technologies). The lack of radionuclides (nuclear medicine / PET) or ionising radiation (nuclear medicine / PET / X-ray CT) makes ultrasonic imaging considerably safer than other methods – 2D or 3D – and allows a patient to be imaged frequently without the fear of an accumulating radiation dose.

Often, an impedance-matching gel is first applied to the patient, to remove air-gaps between their body and the transducer. The transducer is then pressed against this gelled area, and imaging can begin. This is a much quicker and simpler process than MRI, which often requires the injection of contrast agents and an X-ray CT scan† in preparation. While some risks of medical ultrasound have been proposed[‡], the potential risks of ultrasound imaging are still an area of active investigation.

The ability to produce real-time video of processes within the body with ultrasound is rivalled by perhaps only fMRI[‡], and is an invaluable diagnostic tool for checking and identifying heart damage and defects. This, in addition to the unique ability of colour Doppler ultrasound to show the velocities of blood along several blood vessels (or in the chambers of the heart) simultaneously allows ultrasound to provide information that no other current non-invasive imaging technology can.

Advances in ultrasound imaging include new noise-filtering techniques and beam shaping techniques, measurements of tissue elasticity by their nonlinear effects on the sound (harmonic generation) and outside the medical field: ultrasonic pump-probe analysis of semiconductors quantum structures, providing nanometre resolution images.

* A pocket ultrasound scanner is available at <http://www.signosticsmedical.com/>

† To detect metallic objects, which would heat rapidly in the strong pulsing magnetic fields of an MRI scanner – and could potentially be ripped out of the patient, or forced into organs - possibly causing fatal damage.

‡ By distinguishing between oxygenated and deoxygenated blood, fMRI (functional MRI) can indicate the electrical activity within different regions of the brain, in real-time.

6. Table of figures

| | |
|---|----|
| FIGURE 1: "THE HORSE IN MOTION", EADWEARD MUYBRIDGE, POSSIBLY THE FIRST EXAMPLE OF A VIDEO RECORDING..... | 4 |
| FIGURE 2: PULSE-ECHO - REFLECTING A WAVEFRONT OFF A SURFACE, THEN DETECTING THE DEFORMED WAVEFRONT IN ORDER TO CALCULATE THE RELIEF OF THE REFLECTING SURFACE. | 5 |
| FIGURE 3: A-MODE ULTRASOUND OUTPUT..... | 6 |
| FIGURE 4: B-SCAN OF AN INFLAMED BICEP TENDON..... | 6 |
| FIGURE 5: M-MODE MITRAL VALVE..... | 7 |
| FIGURE 6: DOPPLER SHIFT FOR FREQUENCY F_0 , WHEN REFLECTED FROM AN OBJECT MOVING AT ANGLE θ WITH RESPECT TO THE PULSE DIRECTION, AND AT VELOCITY V THROUGH A MEDIUM WHERE THE PULSE PROPAGATES AT SPEED C . THE PULSE IS SHIFTED FROM FREQUENCY F_0 TO F_b . THIS EQUATION ASSUMES THAT THE TRANSMITTER AND THE RECEIVER ARE STATIONARY WITH RESPECT TO THE MEDIUM. | 7 |
| FIGURE 7: DOPPLER SPECTRUM WITH ENVELOPE..... | 8 |
| FIGURE 8: TAKING A TIME-SLICE THROUGH A DOPPLER SPECTRUM..... | 8 |
| FIGURE 9: AN INTENSITY PLOT OF A TIME-SLICE THROUGH THE DOPPLER SPECTRUM IN FIGURE 7/FIGURE 8 IS SHOWN. THE Y-AXIS REPRESENTS THE DOPPLER SHIFT AND THE X-AXIS IS THE INTENSITY OF REFLECTED SOUND AT THAT FREQUENCY. NOTICE THAT THERE ARE A VARIETY OF DIFFERENT VELOCITIES BEING REPORTED, THE VALUES OF WHICH MAY BE ESTIMATED FROM THE Y-AXIS LABELS IN FIGURE 7..... | 8 |
| FIGURE 10: PULSED DOPPLER: IMAGE AND VELOCITY INFORMATION. THE OPERATOR CAN USE THE IMAGE TO INDICATE THE FLOW ANGLE TO THE COMPUTER. | 9 |
| FIGURE 11: COLOUR DOPPLER. A B-MODE IMAGE IS DISPLAYED ABOVE, WITH THE VELOCITY FIELD SUPERIMPOSED AS ARTIFICIAL COLOUR. THE SCALE ON THE LEFT INDICATES THE COLOUR USED FOR VARIOUS VELOCITIES. THE VELOCITY SPECTRUM IS DISPLAYED BELOW THE IMAGE..... | 9 |
| FIGURE 12: A LINEAR ARRAY..... | 10 |
| FIGURE 13: A CURVILINEAR ARRAY..... | 10 |
| FIGURE 14: NEAR FIELD (FRESNEL) REGIME OF LENGTH Z , FROM TRANSDUCER ELEMENT WITH RADIUS R , AND FAR FIELD (FRAUNHOFER) REGIME..... | 11 |
| FIGURE 15: A LINEAR ARRAY WHERE ADJACENT ELEMENTS ARE FIRED IN GROUPS OF TWO. SIX GROUPS ARE POSSIBLE ON THE ILLUSTRATED ARRAY, ALLOWING THE NEAR-FIELD DEPTH TO BE QUADRUPLE THAT OF A SINGLE-ELEMENT ARRAY, WHILE ONLY REDUCING THE LATERAL RESOLUTION BY $1/7$ (14%)..... | 11 |
| FIGURE 16: A LINEAR ARRAY WHERE ADJACENT ELEMENTS ARE FIRED IN GROUPS OF FOUR. FOUR GROUPS ARE POSSIBLE ON THE ILLUSTRATED ARRAY, ALLOWING THE NEAR-FIELD DEPTH TO BE SIXTEEN TIMES THAT OF A SINGLE-ELEMENT ARRAY! THE LATERAL RESOLUTION HOWEVER HAS BEEN REDUCED BY $3/7$ (42%), ALTHOUGH A TYPICAL ARRAY WOULD HAVE CONSIDERABLY MORE THAN SEVEN ELEMENTS!..... | 11 |
| FIGURE 17: SIDE-LOBES – NOTICE THE DARK “BOWEL-LIKE” STRUCTURES [FOLLOW GREEN ARROWS], PRODUCED BY THE SIDE-LOBES REFLECTING OFF THE ACTUAL BOWEL [IMAGED AT THE PURPLE ARROWS]. | 12 |
| FIGURE 18: WAVEFRONT SHAPING BY (A) SHAPED ARRAYS, (B) ACOUSTIC LENS AND (C) PHASED ARRAY (BOXES REPRESENT DELAY)..... | 12 |
| FIGURE 19: PHASED ARRAY FOCUSING THE PULSE. | 13 |
| FIGURE 20: SWEEPING THE BEAM WITH A PHASED ARRAY, BY INTRODUCING AN ASYMMETRIC DELAY TO THE TRANSDUCERS IN ORDER TO SHAPE THE WAVEFRONT..... | 13 |
| FIGURE 21: OFF-AXIS IMAGING WITH A PHASED ARRAY. | 13 |
| FIGURE 22: A 2400-ELEMENT 2D PHASED ARRAY..... | 13 |
| FIGURE 23: DEPTH SELECTION BY FOCUSING. THE BOX CAMERA IS IN FOCUS; THE LENS SURFACE IS NOT. THE ROUGH SURFACE OF THE BOX CAMERA IS CLEARLY VISIBLE. | 14 |
| FIGURE 24: DEPTH SELECTION BY FOCUSING. THE LENS SURFACE IS IN FOCUS; THE BOX CAMERA IS NOT. THE DIRT ON THE LENS IS NOW CLEARLY VISIBLE, WHILE THE CAMERA IS REDUCED TO A DARK BLUR. | 14 |
| FIGURE 25: HIGH SPATIAL FREQUENCIES WERE ONLY RECORDED WHEN THEY ORIGINATED FROM NEAR THE FOCAL PLANE. HENCE THE MOST DETAIL IN THIS FILTERED IMAGE IS ON THE CAMERA AND GUITARS. | 14 |
| FIGURE 26: THE DETAILS OF THE BOX WERE FILTERED BY THE FOCUSING OF THE CAMERA, NOW THE ONLY VISIBLE DETAILS ARE IN THE NEW FOCAL PLANE - THE LENS SURFACE..... | 14 |
| FIGURE 27: DYNAMIC DEPTH FOCUSING..... | 15 |

7. References

- ¹ "History of Ultrasound in Obstetrics and Gynecology, Part 1", <http://www.ob-ultrasound.net/history1.html> (14-May-2011)
- ² "Radar: Early Radar History", <http://www.purbeckradar.org.uk/penlevradararchives/history/introduction.htm> (14-May-2011)
- ³ "Ultrasound attenuation measurement of tissue in frequency range 2.5-40 MHz using a multi-resonance transducer", Kudo, N.; Kamataki, T.; Yamamoto, K.; Onozuka, H.; Mikami, T.; Kitabatake, A.; Ito, Y.; Kanda, H.; , Ultrasonics Symposium, 1997. Proceedings., 1997 IEEE , vol.2, no., pp.1181-1184 vol.2, 5-8 Oct 1997, doi: 10.1109/ULTSYM.1997.661789
- ⁴ "SLAC Linac Coherent Light Source – Multimedia – Video – The Horse in Motion", <http://lcls.slac.stanford.edu/VideoViewMuybridge.aspx> (16-May-2011)
- ⁵ "The Horse in motion", Eadweard Muybridge (c1878), Library of Congress Prints and Photographs Division Washington, D.C. 20540 USA, cph 3a45870 <http://hdl.loc.gov/loc.pnp/cph.3a45870>
- ⁶ "LM555 Timer", National Semiconductor, <http://www.national.com/ds/LM/LM555.pdf> (17-May-2011)
- ⁷ "Small animal diagnostic ultrasound", Thomas G. Nyland, John S. Mattoon, ISBN:0-7216-7788-6 pp.7
- ⁸ "Anaesthesia UK: Types of ultrasound", <http://www.frca.co.uk/article.aspx?articleid=300>, (15-May-2011)
- ⁹ "Musculoskeletal", http://ultrasound-images.com/musculoskeletal.htm#Rib_fracture (15-May-2011)
- ¹⁰ "Basic ultrasound, echocardiography and Doppler ultrasound", <http://internalmed.slu.edu/cardiology/echolab/> (15-May-2011)
- ¹¹ "Blood velocity in human arteries measured by a bidirectional ultrasonic doppler flowmeter", Risøe, C. and Wille, S. (1978), Acta Physiologica Scandinavica, 103: 370–378. doi: 10.1111/j.1748-1716.1978.tb06230.x
- ¹² "Principles of Ultrasound", Dr Tony Evans, Division of Medical Physics, LIGHT Institute
- ¹³ "Bedside Ultrasound for Pneumothorax | Mount Sinai Emergency Medicine Ultrasound", <http://sinaiem.us/tutorials/pneumothorax> (16-May-2011)
- ¹⁴ "Diagnostic Ultrasound: Physics and Equipment", Peter R. Hoskins, Kevin Martin, Abigail Thrush, ISBN: 978-0521757102, pp. 28-38
- ¹⁵ "Radar Basics", <http://www.radartutorial.eu/13.ssr/sr09.en.html> (17-May-2011)
- ¹⁶ "Side lobe artefacts explained", <http://sinaiem.us/artifacts/artifacts-5-on-the-sidelines> (17-May-2011)
- ¹⁷ "A beginner's guide to speckle", <http://dukemil.bme.duke.edu/Ultrasound/k-space/node5.html> (17-May-2011)
- ¹⁸ "Ultrasound Physics", <http://www.wikiradiography.com/page/Ultrasound+Physics> (17-May-2011)
- ¹⁹ "Diagnostic Ultrasound: Physics and Equipment", Peter R. Hoskins, Kevin Martin, Abigail Thrush, ISBN: 978-0521757102, pp. 42
- ²⁰ "Dynamic Focusing of Phased Arrays for Nondestructive Testing: Characterization and Application", <http://www.ndt.net/article/v04n09/lamarre/lamarre.htm> (17-May-2011)
- ²¹ "Ultrasound Affects Embryonic Mouse Brain Development", <http://opac.yale.edu/news/article.aspx?id=1755> (18-May-2011)